Autodetachment Dynamics of Acrylonitrile Anion Revealed by Two-Dimensional Electron Impact Spectra

K. Regeta and M. Allan

Phys. Rev. Lett. **110**, 203201 — Published 13 May 2013

DOI: 10.1103/PhysRevLett.110.203201

Autodetachment dynamics of acrylonitrile anion revealed by 2D electron impact spectra

K. Regeta and M. Allan
Department of Chemistry, University of Fribourg,
Chemin du Musée 9, CH-1700 Fribourg, Switzerland
(Dated: March 21, 2013)

2D electron energy loss spectra of acrylonitrile are presented at the incident energy range 0.095-0.9 eV, where the incoming electron is temporarily captured in the lowest π^* orbital. The cross section is plotted as a function of incident electron energy, that determines which vibrational resonant anion state is populated, and of the electron energy loss, that shows into which final vibrational states each resonance decays. The striking result is that besides the expected horizontal (for given resonances) and vertical (for given final states) patterns of peaks, diagonal arrangements of peaks are observed. They reveal restrictive selectivity with respect to which vibrations are de-excited in the detachment process, with ν_4 (C≡N stretch) and ν_7 (C−H rocking) dominating. Surprisingly, all spectral features could be assigned to vibrational levels of the valence π^* resonance, and none to dipole-bound vibrational Feshbach resonance, although the latter must also exist in this energy range.

PACS numbers:

The interplay of nuclear and electronic motion in autodetachment of transient molecular anions is a fascinating subject and the emitted electron carries information about the motion of the nuclei on the anion potential surface. Autodetachment may proceed with several different mechanisms, depending on the nature of the anion and its energy respective to the neutral [1, 2]. One of them, vibrational autodetachment, is a prototype process where the Born-Oppenheimer approximation is broken. One approach to experimental study of autodetachment is based on vibrational photoexcitation of bound anions and detection of autodetached electrons [3–8], but the autodetaching anions can also be formed by electron attachment [9, 10]. Various aspects of the theory were explained in the work of Simons [2, 11–13], with emphasis on vibrational autodetachment that requires inclusion of non-Born-Oppenheimer coupling, the theory of which has initially been inspired by the work on the related process of vibrational autoionization [14].

In this work we prepare the anions by attachment of free electrons, but substantially enhance the power of this method by recording a 2D electron impact spectrum where cross section, represented by color, is plotted as a function of the incident electron energy, which determines the initial state of the negative ion, and of the energy loss, which carries information about the final state of the neutral molecule. This spectrum yields complete information about the decay channels of many resonances. 2D electron spectra were used in the past to study N_2 [15] and CO_2 [16].

Acrylonitrile CH_2CHCN is a suitable target for this study because electron transmission spectroscopy (ETS) revealed sharp structures – narrow resonances – in electron scattering at low energy [17]. Another interesting aspect of acrylonitrile in connection with the present work is that its large dipole moment (3.86 D) supports a dipole-bound state, with a measured binding energy of 6.9 meV [18–21]. Acrylonitrile thus potentially offers the possibility to study the coexistence of, and interactions between, the dipole-bound and the valence states of an anion [22, 23]. Dissociative electron attachment for acrylonitrile has been measured [24] – the lowest bands have an onset around 2 eV, above the energy range of the present work. The interest in acrylonitrile is augmented by its occurrence in outer space [28] where it may be exposed to free electrons, and because it is a widely used monomer precursor in polymer science.

Methods. The measurements were performed using a spectrometer with hemispherical analyzers [29]. The energy scales are accurate to within ±10 meV, resolution was 16 meV in the energy-loss mode with 300 pA beam current. The 2D spectrum was obtained by recording a series of 160 electron energy-loss (EEL) spectra with constant incident energies in the range 0.095 - 0.9 eV and combining them to a 2D spectrum. Each of the 160 EEL spectra was corrected for the response function of the analyzer and then arbitrarily normalized to 1 at the top of the elastic peak. Since the elastic peak drops with rising incident energy in reality, normalizing it to 1 enhances somewhat the signal at higher incident energies, and improves visibility. Spectra were recorded at the scattering angle of 135° to emphasize resonant processes and reduce the extent of direct excitation in the spectrum. All calculated quantities given in this paper were obtained with density functional theory (DFT) at the B3LYP/6-311++G(2df,2p) level, with the Firefly code [30], based partly on GAMESS [31].

Results. The 2D EEL spectrum shown in Figure 1 plots the differential cross section (DCS), represented by color, as a function of the electron energy loss ΔE and of the incident electron energy E_i. The elastic peak has $\Delta E = 0$ and gives rise to the red vertical ridge on the

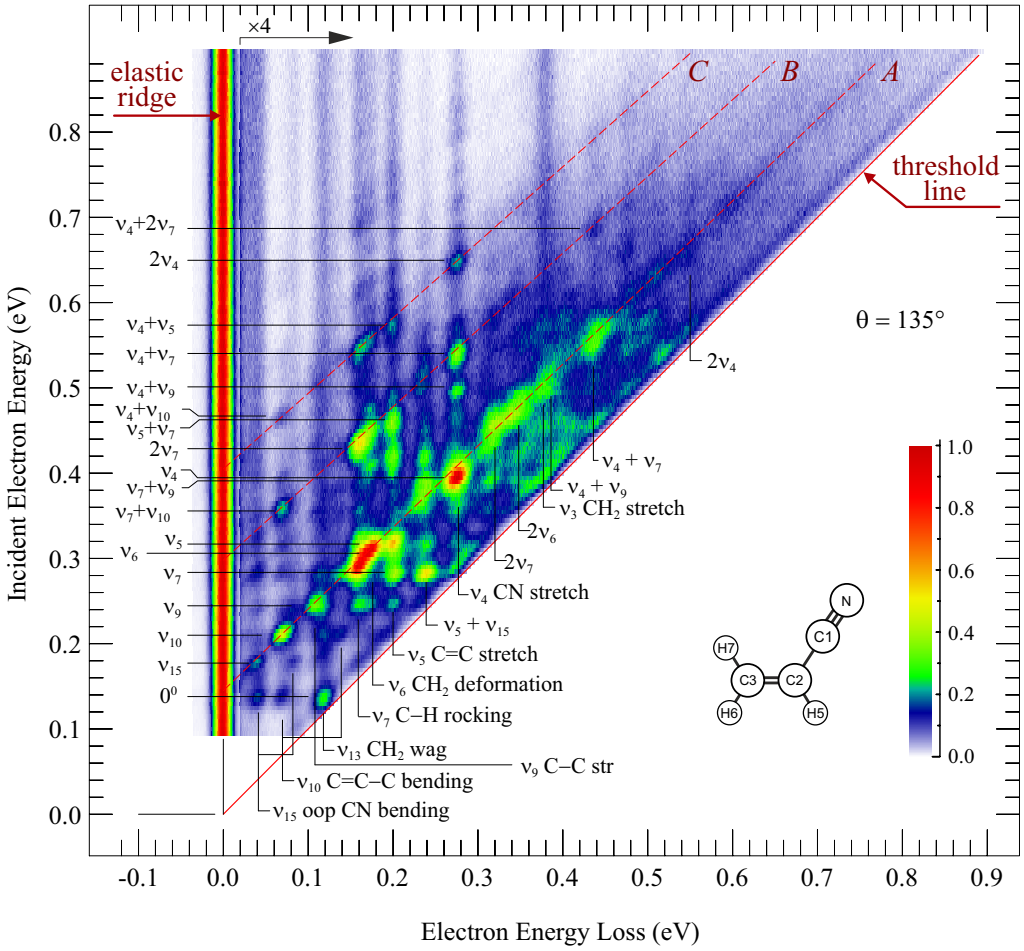

FIG. 1: (Color online) Two-dimensional electron energy loss spectrum of acrylonitrile.

left. The largest possible ΔE is equal to E_i for each incident energy and corresponds to the situation where all the energy of the incident electron is used for internal excitation of the acrylonitrile target and the electron leaves with nearly zero kinetic energy. At this point the excitation of the final state is at its threshold and this situation is encountered along the diagonal *threshold line* drawn red in the Figure.

Excitation of a given *final vibrational state* of the neutral acrylonitrile occurs at a given ΔE for various E_i and gives thus rise to a group of peaks (dots) arranged *vertically* at the corresponding energy loss. The excitation is predominantly resonant, and since acrylonitrile is known to have narrow structures of vibrational origin in the lowest π^* shape resonance [17], the cross section has peaks at the discrete energies of the resonances. A given *resonance* (vibrational state of the transient acrylonitrile anion) decays, with some selectivity, into various vibrations, and these decay channels give rise to a group of peaks (dots) arranged *horizontally* at the incident energy equal to the energy of the resonance.

The two expected features in the 2D spectrum in Figure 1 are thus *vertical* rows of dots, each row corresponding to a given final vibrational state and *horizontal* rows of dots, each row corresponding to a given resonance. The striking observation of this paper are the patterns of *diagonally* arranged dots. The three most prominent diagonal rows are marked by the red dashed lines A, B, C in Figure 1. The rows are nearly, but not exactly, parallel to the threshold line, slowly approaching it with increasing E_i. A quantity common to all dots on a given diagonal is their horizontal shift from the threshold line – it is the residual energy of the scattered electron $E_r = E_i - \Delta E$. The diagonal groups of peaks thus reveal a propensity for discrete residual energies. This is unexpected because residual energy is not directly related to either of the two important quantities of the present experiment – energy of a resonance and energy of the final state.

Assignment of the final vibrational states. The assignment of the individual vibrations is indicated by vertical bars and labels in the lower part of Figure 1. The bars are drawn at energy-losses equal to the vibra-

tional frequencies of neutral acrylonitrile [32]. The π^* orbital where the incoming electron is temporarily captured is antibonding with respect to the C≡N and C=C bonds, making them longer and reducing the vibrational frequencies (Table I), thus providing a force for excitation of ν_4 and ν_5, explaining their prominence in Figure 1. The lowering of the frequencies ν_6 and ν_7 in the anion (Table I), also indicates change of bonding along these modes and rationalizes their substantial intensity in the spectrum. The appreciable intensity of the A'' out-of-plane (oop) vibrations is initially not understandable because both acrylonitrile and its anion are calculated to be planar. The dramatic lowering of the frequencies ν_{12} and ν_{13} (unresolved in the spectrum) indicates that the acrylonitrile anion is 'on the verge of becoming pyramidal' on the C2 and C3 carbons (see insert in Figure 1 for numbering), the potential curves along these two modes become flat in the anion, and this change drives the vibrational excitation.

Assignment of resonances. Assignment of the resonances is indicated on the left of Figure 1. It was obtained by finding a match of the observed spectral features with the calculated vibrational frequencies of the acrylonitrile *anion* listed in Table I. The energy of the origin of the anion vibrational grid is the adiabatic electron attachment energy of acrylonitrile and is *a priori* not known. To determine it, the calculated vibrational grid was moved along the vertical axis until a good match with experimental vertical position of the dots was obtained, identifying the horizontal row of three dots at $E_i = 0.138 \pm 0.01$ eV as the ground vibrational level 0^0 of the anion – the anion is thus adiabatically slightly unbound. This number is in good agreement with the value of +0.11 eV derived from an electron transmission spectrum (ETS) by Burrow *et al.* [17].

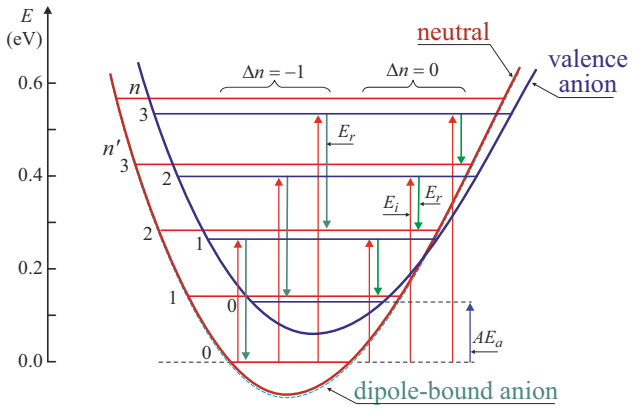

FIG. 2: (Color online) Schematic potential curves.

The diagonal patterns. The schematic potential curves in Figure 2 show that a given residual energy is associated with a given *change* of vibrational quantum $\Delta n = n - n'$, the lowest E_r being associated with $\Delta n = 0$ for all n. The residual energy associated with $\Delta n = 0$ depends only on AE_a. E_r of the $\Delta n = 0$ transitions is the same for all modes N and they are arranged along the diagonal A in Figure 1. When the detachment is regarded as a half-collision, then this half-collision could be called 'vibrationally elastic' along the diagonal A, since n and n' are equal.

Figure 2 shows that this diagonal, extrapolated to $\Delta E = 0$, should cross the 'elastic ridge' at $E_i = AE_a$ and this expectation is confirmed by the experiment in Figure 1. Figure 2 further shows that E_r should decrease slowly with increasing quanta, the rate of decrease being proportional to the difference of the neutral and anion vibrational energies $\Delta\nu = \nu - \nu'$. The diagonal A should thus slowly approach the threshold line – an expectation confirmed by the experiment.

All dots along the diagonal A can be satisfactorily assigned to specific transitions. Designating the transitions as $N^n \rightarrow N'^{n'}$ where N and N' are the labels of the modes and n and n' number of quanta of the anion and the neutral, respectively, the leftmost dot is due to the transition $15^1 \rightarrow 15^1$, the next as $10^1 \rightarrow 10^1$, and similarly for many other modes. Note that dots due to the modes ν_4, ν_5, and ν_7 are slightly below the diagonal because the anion frequencies for these modes are measurably lower than those of the neutral molecule. Dots on the right of the diagonal A are due to transitions where there is more vibrational energy in the neutral than in the anion – a 'vibrationally inelastic' half-collision. Examples are the peaks $0^0 \rightarrow 15^1$, $0^0 \rightarrow 13^1$, $15^1 \rightarrow 15^2$, $9^1 \rightarrow 7^1$, $7^1 \rightarrow 5^1$ and $7^1 \rightarrow 5^1 15^1$.

Dots on the left of the diagonal A are due to transitions where there is less vibrational energy in the neutral than in the anion – the 'vibrationally superelastic' half-collisions. Vibrational energy is converted to electronic energy of the departing electron and the process is in that sense related to the vibrational autodetachment studied on nitroalkanes [3] and other anions [4–8] except that in those cases the anions were electronically bound (for example nitromethane by 172 meV) and vibrational de-excitation was *required* for the electron to leave; in the present case it is optional and is in competition with the $\Delta n = 0$ case. Figure 2 shows that for these transitions, with $\Delta n < 0$, the vertical separation of a given dot from its pendant on the diagonal A is equal to the frequency of the vibration which is de-excited. Figure 1 shows that out of the many modes two are dominant, with peaks arranged along two diagonals, labeled B and C.

All dots can be assigned to specific transitions. Examples on the diagonal B are $7^1 10^1 \rightarrow 10^1$, $7^2 \rightarrow 7^1$ and $4^1 7^1 \rightarrow 4^1$. The vibration de-excited is clearly ν_7. Examples on the diagonal C are $4^1 10^1 \rightarrow 10^1$, $4^1 7^1 \rightarrow 7^1$, $4^1 5^1 \rightarrow 5^1$, $4^2 \rightarrow 4^1$ and the vibration de-excited is ν_4. There are also weaker dots corresponding to de-excitation of ν_9 (e.g., $4^1 9^1 \rightarrow 4^1$) and weak dots at even higher energies which can be assigned to a simultaneous de-

TABLE I: Observed [32] and calculated (scaled by a factor of 0.97) vibrational frequencies of acrylonitrile and its anion (in meV).

			neutral		anion
No	Sym	Type	obs	calc	calc
ν_1	A'	(C−H) asym. str of CH_2	387	392	387
ν_2		(C−H) str of C−H	382	382	377
ν_3		(C−H) sym. str of CH_2	377	378	376
ν_4		C≡N str	278	280	257
ν_5		C=C str	200	201	179
ν_6		CH_2 scissoring	176	174	168
ν_7		C−H rock	159	159	146
ν_8		CH_2 rock	136	134	131
ν_9		C−C str	108	106	107
ν_{10}		C=C−C bend	n.o.	70.2	72.0
ν_{11}		C−C≡N bend	28.4	29.2	28.9
ν_{12}	A''	C−H wag (C2 pyram)	121	121	69.5
ν_{13}		CH_2 wag (C3 pyram)	118	120	24.7
ν_{14}		C=C torsion (C2 pyram)	84.7	85.7	59.6
ν_{15}		oop C−C≡N bend	41.3	42.0	39.3

excitation of ν_4 and ν_7.

Discussion and Conclusions. The 2D spectrum reveals diagonal patterns of the cross section peaks, which are not evident in the more conventional presentation of cross sections. The dominant process is $\Delta n = 0$ – no change of vibrational quanta during the detachment – leading to the diagonal A in Figure 1. Extrapolation of this diagonal to energy loss $\Delta E = 0$ yields the adiabatic electron attachment energy AE_a. Many of the remaining peaks are arranged along two other diagonals (B and C), indicating that a large fraction of the remaining processes are accompanied by a highly selective vibrational de-excitation, dominated by only two modes, ν_7 (C(2)−H(5) rocking) and ν_4 (C≡N stretch).

The results pose two questions – what is the nature of the resonances and of the autodetachment process. As already pointed out by Burrow *et al.* [17], the observed vibrational origin at +0.138 eV belongs to a shape resonance with a temporary electron capture in the lowest π^* orbital. The present analysis could assign all observed spectral features to various vibrational states of this shape resonance. This is surprising in the sense that a dipole-bound negative ion has been observed [19] and calculated [20, 21], and there is no doubt that vibrationally excited states of this dipole-bound anion are vibrational Feshbach resonances (VFR) [10], which should be accessible by the present experiment. Their absence in the spectra may reflect low energy-integrated transition probability, possibly related to narrow widths.

With regard to the second question, Simons [12] showed that for a slightly unbound state like the present shape resonance two mechanisms may compete. One is via the direct electronic process, which involves a conventional anion-neutral Franck-Condon factor, weighted by how much the wave function of a given mode samples areas of the potential surface with large widths $\Gamma(Q)$. The other is the surface jumping route which proceeds via non-Born-Oppenheimer couplings (and which is the only route for vibrational autodetachment of anions like NH^- which are electronically bound [3–8]). This route does not involve Franck-Condon factors and is similar to the vibrational autoionization which, for potential curves of the same shape leads to a $\Delta n = \pm 1$ rule [14]. The $\Delta n = 0$ transitions (on the diagonal A) must thus be dominated by the direct electronic process. The $\Delta n = -1$ processes (diagonals B and C) are much stronger than the $\Delta n = -2$ processes, and thus follow the $\Delta n = \pm 1$ rule. The propensity rules formulated for the non-Born-Oppenheimer route by Simons [1, 2, 12, 13, 33] are not easy to apply qualitatively to decide whether they can explain the striking ν_4 and ν_7 selectivity of the $\Delta n = -1$ detachment.

It is interesting to compare the present results with the resonant photodetachment experiments [3–8]). The initial steps are different but the detachment is the same. There are important differences, however – photoexcitation is capable of reaching even very narrow resonances, which are not well visible in the electron collision experiment because of low attachment probability and the IR selection rules limit the number of observable resonances in the photodetachment experiment.

Outlook. 2D electron energy-loss spectra appear to be a powerful and under-appreciated tool to study nuclear dynamics of anions. It would be interesting to apply the present method to larger molecules, where the 'unselective' or 'unspecific' vibrational excitation related to IVR (intramolecular vibrational redistribution) [34] is operative near threshold, and would thus appear near the threshold line in the 2D spectrum. It would be interesting to apply the present method to molecules where the dissociative electron attachment channel is also open. IR photodetachment experiment on the dipole bound acrylonitrile anion would be interesting – it may provide information on the dipole-bound vibrational Feshbach resonances, which are 'dark' in the present experiment. Calculations addressing both the direct electronic and the non-Born-Oppenheimer paths, and both the valence and the VFR anion states, are desirable.

Acknowledgment. This research is part of project No. 200020-144367/1 of the Swiss NSF.

[1] J. Simons, J. Phys. Chem. A **112**, 6401 (2008).
[2] J. Simons, Adv. Ser. Phys. Chem. **10B**, 958 (2000).
[3] C. L. Adams, H. Schneider, and J. M. Weber, J. Phys. Chem. A **114**, 4017 (2010).
[4] C. L. Adams, B. J. Knurr, and J. M. Weber, J. Chem. Phys. **134**, 064307 (2012).
[5] D. M. Neumark, K. R. Lykke, T. Andersen, and W. C. Lineberger, J. Chem. Phys. **83**, 4364 (1985).
[6] K. R. Lykke, D. M. Neumark, T. Andersen, V. J. Trapa, and W. C. Lineberger, J. Chem. Phys. **87**, 6842 (1987).
[7] S. T. Edwards, M. A. Johnson, and J. C. Tully, J. Chem. Phys. **136**, 154305 (2012).
[8] H. K. Gerardi, A. F. DeBlase, C. M. Leavitt, X. Su, K. D. Jordan, A. B. McCoy, and M. A. Johnson, J. Chem. Phys. **136**, 134318 (2012).
[9] G. J. Schulz, Rev. Mod. Phys. **45**, 423 (1973).
[10] H. Hotop, M.-W. Ruf, M. Allan, and I. I. Fabrikant, Adv. At. Mol. Opt. Phys. **49**, 85 (2003).
[11] P. K. Acharya, R. A. Kendall, and J. Simons, J. Am. Chem. Soc. **106**, 3402 (1984).
[12] J. Simons, J. Am. Chem. Soc. **103**, 3971 (1981).
[13] J. Simons, J. Chem. Phys. **117**, 9124 (2002).
[14] R. S. Berry, J. Chem. Phys. **45**, 1228 (1966).
[15] T. Reddish, F. Currell, and J. Comer, J. Phys. E: Sci. Instrum. **21**, 203 (1988).
[16] F. Currell and J. Comer, Phys. Rev. Lett. **74**, 1319 (1995).
[17] P. D. Burrow, A. E. Howard, A. R. Johnston, and K. D. Jordan, J. Phys. Chem. **96**, 7570 (1992).
[18] C. Desfrançois, H. Abdoul-Carime, N. Khelifa, and J. P. Schermann, Phys. Rev. Lett. **73**, 2436 (1994).
[19] L. Suess, Y. Liu, R. Parthasarathy, and F. B. Dunning, J. Chem. Phys. **119**, 808 (2003).
[20] G. L. Gutsev and L. Adamowicz, J. Phys. Chem. **99**, 12890 (1995).
[21] G. L. Gutsev and L. Adamowicz, Chem. Phys. Lett. **235**, 377 (1995).
[22] R. N. Compton, H. S. Carman, C. Desfrançois, H. Abdoul-Carime, J. P. Schermann, J. H. Hendricks, S. A. Lyapustina, and K. H. Bowen, J. Chem. Phys. **105**, 3472 (1996).
[23] T. Sommerfeld and S. Knecht, Eur. Phys. J. D **35**, 207 (2005).
[24] M. Heni and E. Illenberger, Int. J. of Mass Spectrom. and Ion Proc. **73**, 127 (1986).
[25] J. Tornero, H. Telle, G. García, and A. G. Ureña, PCCP **13**, 8475 (2011).
[26] Y. Fukuda, M. Ichihashi, A. Terasaki, T. Kondow, K. Osoda, and K. Narasaka, J. Phys. Chem. A **105**, 7180 (2001).
[27] K. Ohshimoa, F. Misaizub, and K. Ohno, Eur. Phys. J. D **24**, 339 (2003).
[28] F. F. Gardner and G. Winnewisser, Astrophys. J. **195**, 127 (1975).
[29] M. Allan, Phys. Rev. A **81**, 042706/1 (2010).
[30] A. A. Granovsky, *Firefly version 8.0.0*, `http://classic.chem.msu.su/gran/firefly/index.html`.
[31] M. W. Schmidt, K. K. Baldridge, J. A. Boatz, S. T. Elbert, M. S. Gordon, J. H. Jensen, S. Koseki, N. Matsunaga, K. A. Nguyen, S. Su, et al., J. Comput. Chem. **14**, 1347 (1993).
[32] J. M. Alía, H. G. M. Edwards, W. R. Fawcett, and T. G. Smagala, J. Phys. Chem. A **111**, 793 (2007).
[33] G. Chalasinski, R. A. Kendall, H. Taylor, and J. Simons, J. Phys. Chem. **92**, 3086 (1988).
[34] M. Allan, J. Electron Spectrosc. Relat. Phenom. **48**, 219 (1989).